한국항해항만학회지 제47권 제2호
J. Navig. Port Res. Vol. 47, No. 2 : 106-119, April 2023 (ISSN:1598-5725(Print)/ISSN:2093-8470(Online))
DOI : http://dx.doi.org/10.5394/KINPR.2023.47.2.106

Design and Analysis of a Novel Methanol SOFC Combined System for Marine Applications Toward Future Green Shipping Goals

Duong Phan Anh · Ryu Bo Rim** · † Hokeun Kang*

**Postdoctoral Researcher, Department of Marine System Engineering, Korea Maritime and Ocean University*
***PhD.Candidate, Department of Marine System Engineering, Korea Maritime and Ocean University*
† Professor, Division of Coast Guard Studies, Korea Maritime and Ocean University

Abstract : *Due to global decarbonization movement and tightening of maritime emissions restrictions, the shipping industry is going to switch to alternative fuels. Among candidates of alternative fuel, methanol is promising for decreasing SOx and CO2 emissions, resulting in minimum climate change and meeting the goal of green shipping. In this study, a novel combined system of direct methanol solid oxide fuel cells (SOFC), proton exchange membrane fuel cells (PEMFC), gas turbine (GT), and organic Rankine cycle (ORC) targeted for marine vessels was proposed. The SOFC is the main power generator of the system, whereas the GT and PEMFC could recover waste heat from the SOFC to generate useful power and increase waste heat utilizing efficiency of the system. Thermodynamics model of the combined system and each component were established and analyzed. Energy and exergy efficiencies of subsystems and the entire system were estimated with participation of the first and second laws of thermodynamics. The energy and exergy efficiencies of the overall multigeneration system were estimated to be 76.2% and 30.3%, respectively. The combination of GT and PEMFC increased the energy efficiency by 18.91% compared to the SOFC stand-alone system. By changing the methanol distribution ratio from 0.05 to 0.4, energy and exergy efficiencies decreased by 15.49% and 5.41%, respectively. During the starting up and maneuvering period of vessels, a quick response from the power supply system and propulsion plant is necessary. Utilization of PEMFC coupled with SOFC has remarkable meaning and benefits.*

Key words : *methanol, SOFC, PEMFC, thermodynamics analysis, ORC*

1. Introduction

Over 80% of international cargos trade is transported over the sea, making maritime transport the most energy-efficient route of cargo transportation (Zis et al., 2020)(R. Li et al., 2022). Maritime transport is essential for global trade and significantly contributes to sustainable development worldwide (Wang et al., 2020). The shipping transportation is necessary for decarbonization, which is at the top of the domestic and international policy agenda (Xing et al., 2021). The International Maritime Organization (IMO) has launched numerous regulations and guidelines to regulate airborne pollutants and restrict greenhouse gas emissions (GHGs) such as the IMO Initial Strategy, MARPOL, etc. The strategy includes a commitment to minimize CO_2 emissions per transport work by over 40% by 2030 and reduce total GHG emissions from maritime transportation by over 50% from 2008 levels by 2050 (International Maritime Organzation)(Hansson et al., 2020). To assist reducing GHG emissions from shipping, it is necessary to switch to alternative low-and/or zero-carbon fuels because technical and operational efficiency measures alone will not be able to achieve the desired emissions reduction (Ashrafi et al., 2022). Several prospective decarbonization marine fuel alternatives, including liquefied natural gas (LNG), hydrogen, ammonia, biofuel, and methanol, are available to the shipping industry to assist in the reduction of emissions. Among them, methanol is prospective and promising as a hydrogen fuel source with a high hydrogen content. It is also a potential and promising maritime fuel for lowering SOx and CO_2 emissions, resulting in minimal climatic changes and green shipping strategies (Valera-Medina et al., 2021).

Methanol (CH_3OH) is a colorless, clear substance that is flammable, unstable, and has an alcoholic odor. Methanol is a polar organic solvent that is well known for being toxic. According to Adamson et al. (Adamson and Pearson, 2000) methanol is still advised, nevertheless, because it is extremely safe compared to other hydrogen transporters and fuels. The liquid form of methanol is simple to handle

† Corresponding author, hkkang@kmou.ac.kr 051)410-4260
* anhdp@g.kmou.com
** ruyborim@g.kmou.ac.kr

and has a boiling point of 64.7 ℃, high energy density, high octane rating (Wang et al., 2019), and it is environmentally friendly(Kulikovsky, 2008). Methanol is also safe to handle at normal temperatures and pressures, is convenient to store, and easy to refuel (Atacan et al., 2017)(Calabriso et al., 2015). As a result, methanol is a suitable fuel option for fuel cells as well as other nautical applications such as internal combustion engines, gas turbines (Alias et al., 2020).

Researchers and manufacturers are looking at methanol coupled with fuel cells because of its advantages over internal combustion engines, including high efficiency, less noise, less air pollution, and higher thermodynamic performance. Methanol can be either directly or indirectly delivered to fuel cells depending on the kind and operating temperature of the fuel cells. The SOFC and PEMFC are the two most popular fuel cells designs that can be used with methanol systems. The limitation experimental findings have been published for other types of fuel cells, such as using alkaline and alkaline membranes (Hansson et al., 2020). Methanol can be reformed at a lower temperature (about 250 °C) than other fuel sources because of its molecular properties (Zhao et al., 2022). PEMFCs indirectly use methanol by reforming (Sankar et al., 2017)(Chen et al., 2011), whereas SOFCs directly use methanol (Kim et al., 2007)(Bicer and Khalid, 2020). There have been several studies on methanol as a fuel and its use in maritime fuel cells due to its enormous potential to be paired with SOFC and PEMFC.

(Laosiripojana and Assabumrungrat, 2007) experimented with a direct methanol SOFC system over Ni/YSZ anode at an operating temperature from 900 – 975 ℃. The research shown that methanol can be efficiently supplied to SOFC without any carbon formation. The methanol reformation rate was obtained at 100% if the operating temperature of the SOFC close to 900 ℃. (Kim et al., 2007) investigated the stability and performance of direct methanol SOFC with Cu-ceria-YSZ and carbon-ceria-YSZ as anode and demonstrated that methanol is more effectively oxidized in compared with H_2 over tested anodes materials. The findings shown that, even at very low temperatures, species within SOFC electrodes can be highly migratory. (Zhang et al., 2022) experimented with the effects of the catalyst layer on the operation of a direct methanol SOFC system. The enhanced electrochemical performance proves that the integrated catalyst layer is helpful in catalytic the methanol fuel for Ni-YSZ anode-supported SOFCs. The reforming ability of the integrated catalyst layer for methanol is studied by analyzing the microstructural and composition of the anode and catalyst layer after the stability test. The integrated catalysts layer shows a 55.2% reduction in polarization resistance and 42.32% increase in peak power density at 800 °C after the inclusion of the integrated catalyst layer. (Y. Li et al., 2022) analyzed the performance of indirect methanol high temperature proton exchange membrane fuel cells (HT-PEMFC) and revealed that methanol is thought to be an ideal fuel for PEMFC due to its high hydrogen to carbon ratio and lack of carbon-to-carbon (C-C) bonds. The developed model could achieve an 8.8% exergy utilization factor, a 47.24% trigeneration primary energy saving, and a 66.3% energy efficiency. The conversion of CH_3OH and the hydrogen production are more than 95% in the acceptable temperature range when the H_2O/CH_3OH mole ratio is greater than 1.2. (Özcan and Akın, 2019) optimized the methanol steam reforming process for the indirect methanol HT-PEMFC system. The appropriate temperature, pressure, and H_2O/MeOH ratio to produce hydrogen for HT-PEMFC were determined to be 246 ℃, 1 atm, and 5.6, respectively. Additionally, at these ideal conditions, carbon monoxide production in all three scenarios is extremely minimal, between 30 and 1700 ppm, and is therefore acceptable to the anode catalysts of HT-PEMFC systems. The SOFC combined system for marine application was studied by (Duong et al., 2022b). The study showed that the energy and exergy efficiencies of combined system can be obtained 64.53% and 61.14%, respectively. The waste heat recovery systems increased 20.73% energy efficiency in comparison to the SOFC stand-alone system. However, because SOFC operated at high temperatures (from 700 to 1000 ℃), it was unsuitable for marine vessels that required rapid response of the propulsion system and electric power during start-up and maneuvering.

It would be excellent if hydrogen could be extracted from methanol utilizing waste heat from SOFC and pressure swing adsorption (PSA) and supply to the PEMFC. This would boost the fuel cells system's overall energy efficiency. It denotes the usage of a methanol SOFC as the system's main power source, with the waste heat from its exhaust gas being repurposed as a heat source for a system that transforms and purifies methanol to produce more hydrogen for a PEMFC. The hydrogen storage and PEMFC system will instantly produce power for the propulsion plant thanks to the low working temperature of

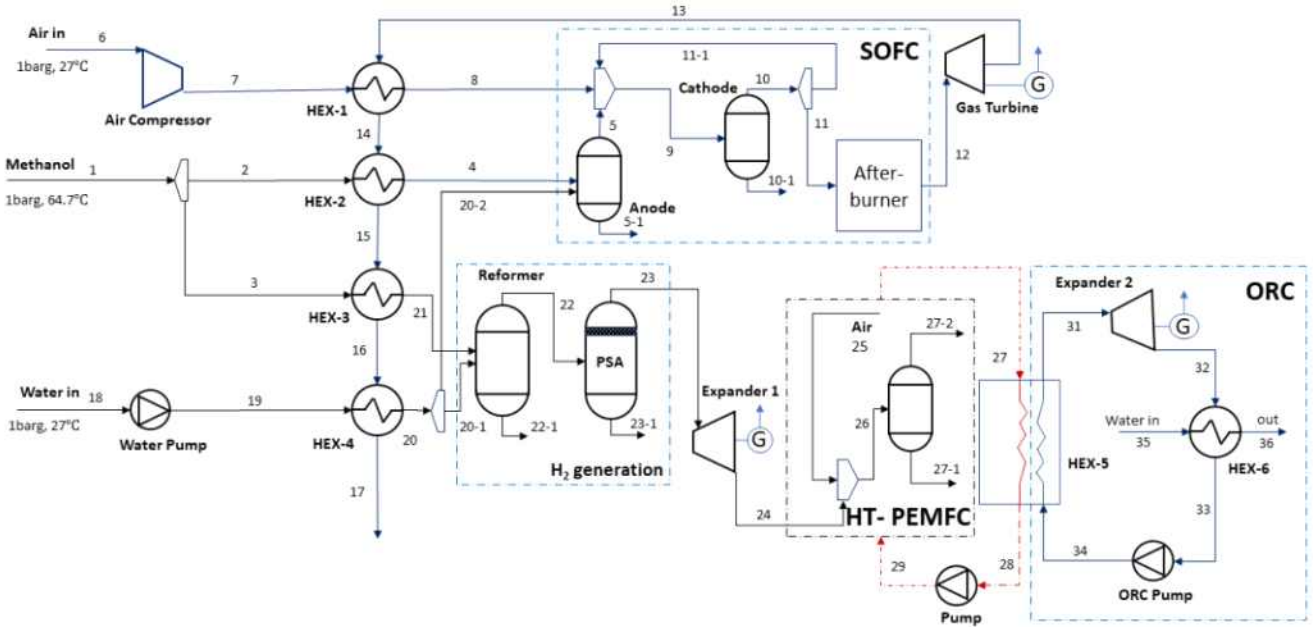

Fig. 1 Configuration of the designated methanol-powered SOFC-GT -PEMFC-ORC

PEMFC, whilst SOFC, which runs at a higher temperature, will largely be used under stable seagoing circumstances. The methanol used as a marine fuel in this study is a proposed and assessed innovative combined SOFC-GT-PEMFC system. The main contributions of current research are listed below:

- Use of methanol as green fuel source for marine vessels;
- Designation and analysis of novel combined system SOFC-GT-PEMFC-ORC;
- A thorough analysis of the methanol-reforming and purifying systems;
- Designates an exhaust heat harvesting system for enhancing the thermodynamic efficiencies of systems;
- Comprehensive analysis of the influence of methanol distribution ratio on the efficiencies of system.

2. System description

A general cargo vessel with an electric propulsion system of 3800 kW was targeted to application. The vessel operates on the Yellow Sea, is 130 m long and has 3800 gross tonnage.

The propulsion plant's main power source is referred to as the SOFC. The core idea behind the phrase "integrated system" is the utilization of waste heat from SOFCs to generate useful work (electricity). A PEMFC is an auxiliary power source that gives the system surplus power, especially during maneuvering and loading/unloading. The high-temperature exhaust heat of SOFC will be reused in turn by three regenerators and a methanol dissociation unit (MDU). The HT-PEMFC is selected in this system to produce extra energy from pure hydrogen. For HT-PEMFC, triethylene glycol is used as the cooling oil. The organic Rankine cycle (ORC) transfers heat from the HT-PEMFC's oil used for cooling to its operating fluid. Their expander devices provide electricity for these procedures.

The proposed integrated SOFC-GT-PEMFC-ORC system is shown in Fig 1. The fuel gas supplies system (FGSS) supply the SOFC combined system with methanol. Due to different operating temperatures and working characteristics, methanol is directly supplied to SOFC, whereas indirect supply to PEMFC via H_2 generation system that includes methanol reforming system (MR) and pressure swing adsorption (PSA). The main electrochemical reaction will be taken in the SOFC. After that, the exhaust gas is delivered to the afterburner to finish the combustion process. The temperature of the exhaust gas increased because of the significant amount of heat produced. The exhaust gas is subsequently used to generate extra energy in regenerative and gas turbines (GT). As a result, a number of regenerators use and transport SOFC waste heat. The fundamental elements and guiding principles of the cycles are described below:

SOFC: The two heat exchangers pre-heat methanol and compressed air in sequence using the SOFC's exhaust gas.

By this way, the compressed air and methanol can be obtained at the SOFCs' needed input temperature. In the SOFC, reforming and electrochemical reactions take place after preheating. These reactions produce a significant amount of heat and electrical energy (resulting from converting chemical energy to electrical energy). The ship's propulsion system then receives the AC electricity that was first converted from DC.

H_2 generation system: Using a suitable catalyst in the reformer, a methanol-water mixture can be transformed into reformate gas. The CuZn-base, which is highly active at low temperatures and reasonably priced, is taken into consideration as a catalyst in this study. The production gas, which is created by reforming methanol and consists of water vapor, carbon dioxide, hydrogen, and carbon monoxide, is then fed to the PSA, where pure hydrogen is separated from the other produced gases.

PEMFC system: The separated pure hydrogen (stream 24) is provided to the HT-PEMFC after being reduced in pressure by expander 1 to the working pressure of the HT-PEMFC. The electrochemical reaction will take place in cathode of HT-PEMFC. Those reaction produce electricity and heats. Heat is supplied to the ORC which transfers heat from the cooling oil of the HT-PEMFC via HEX-7. Heat from cooling oil in the evaporator vaporizes the organic working fluid. The expander is powered to produce energy by the superheated steam that enters it from the organic working fluid (stream 37). The organic working fluid's steam condenses in the condenser before going into the ORC pump (HEX-8). The ORC Pump supplies the working fluid to obtain the required pressure prior to starting the cycle.

3. Thermodynamic investigation

3.1 Thermodynamic balance equations

The mass and energy, entropy balance, and exergy destruction are general thermodynamic balance equations covered in this section. Thermodynamic modelling and analysis are addressed in detail using methods for analyzing energetic and exergetic efficiencies. The factors for the thermodynamic analysis of a thermal system are also provided. The model that is being provided is predicated on the following:

- It is envisaged that the entire system will function in a steady-state;
- Environment with minimal changes in kinetic and potential energy;
- It is envisioned that heat is maintained through the connecting of the pipes;
- The drops in pipeline pressure are not taken into account.

Mass balance equation:

Under steady-state, four equilibrium equations are created and explored for mass, energy, entropy, and exergy. The rate of mass is unchanged in the control volume (CV) under the steady-state (Al-Hamed and Dincer, 2021):

$$\sum_{in}\dot{m}_{in} = \sum_{out}\dot{m}_{out} \tag{1}$$

$$\sum_{in}\dot{m}_{in} - \sum_{out}\dot{m}_{out} = \frac{dm_{CV}}{dt} = 0 \tag{2}$$

where $\dot{m}$ stand for mass flow rate (kg/h).

- Energy balance:

$$\sum_{in}\dot{m}_{in}h_{in} + \dot{Q}_{in} + \dot{W}_{in} = \sum_{out}\dot{m}_{out}h_{out} + \dot{Q}_{out} + \dot{W}_{out} \tag{3}$$

$$\dot{Q} - \dot{W} + \sum_{in}\dot{m}_{in}\left(h_{in} + \frac{V_{in}^2}{2} + gZ_{in}\right) - \sum_{out}\dot{m}_{out}\left(h_{out}\frac{V_{out}^2}{2} + gZ_{out}\right) = 0 \tag{4}$$

Based on the first law of thermodynamics (Al-Hamed and Dincer, 2019)

where $\dot{Q}$, $\dot{W}$ and h represent the heat transfer rate, mechanical power and specific enthalpy of the fluid, respectively.

The precise kinetic and potential energy connected to the entering and exiting mass flow rates in this thermodynamic investigation were ignored and thought to be insignificant (Al-Hamed and Dincer, 2021):

$$\dot{Q}_{in} + \sum_{in}\dot{m}_{in}(h_{in}) = \dot{W}_{out} + \sum_{out}\dot{m}_{out}(h_{out}) \tag{5}$$

- Entropy and exergy balance:

Based on the second law of thermodynamics: The rate of change entropy in CV is zero under steady-state conditions.

$$\sum_{in}\dot{m}_{in}S_{in} + \sum\left(\frac{\dot{Q}}{T}\right) + \dot{S}_{gen} = \sum_{out}\dot{m}_{out}S_{out} \tag{6}$$

$$\sum_{k}\frac{\dot{Q}_k}{T_k} + \sum_{in}\dot{m}_{in}(s_{in}) + \dot{S}_{gen} - \sum_{out}\dot{m}_{out}(s_{out}) = \frac{dS_{CV}}{dt} = 0 \tag{7}$$

or

$$\sum_k \frac{\dot{Q}_k}{T_k} + \sum_{in} \dot{m}_{in}(s_{in}) + \dot{S}_{gen} = \sum_{out} \dot{m}_{out}(s_{out}) \quad (8)$$

where T, $\dot{S}_{gen}$, and s denote the temperature (°C), specific entropy and the entropy of the thermal process, respectively.

- The change of exergy.

$$\sum_k \left(1 - \frac{T_0}{T_k}\right)\dot{Q}_k - \dot{W}_{out} + \sum_{in} \dot{m}_{in}(ex_{in}) - \sum_{out} \dot{m}_{out}(ex_{out}) - \dot{E}x_{dest} = \frac{dEx_{CV}}{dt} = 0 \quad (9)$$

$$\sum_k \left(1 - \frac{T_0}{T_k}\right)\dot{Q}_k + \sum_{in} \dot{m}_{in}(ex_{in}) = \sum_{out} \dot{m}_{out}(ex_{out}) + \dot{W}_{out} + \dot{E}x_{dest} \quad (10)$$

- Specific exergy and the exergy destruction rate:

The entropy production rate is employed to calculate the exergy destruction rate.

$$\dot{E}x_{dest} = T_0 \dot{S}_{gen} \quad (11)$$

Here, T_o, $\dot{E}x_{des}$ and ex denote the ambient temperature (°C), exergy destruction rate and the specific exergy of the fluid, respectively.

The specific exergy values:

$$ex_j = ex_j^{ph} + ex_j^{ch} + ex_j^{ke} + ex_j^{pe} \quad (12)$$

The kinetic and potential exergy were found to be insignificant in this thermodynamic analysis and were so disregarded. Using a weighted average method appropriate for ideal gas combinations, the specific enthalpy and entropy of SOFC exhaust gases were computed.

$$ex_j = ex_j^{ph} + ex_j^{ch} \quad (13)$$

The physical exergy:

$$ex_j^{ph} = (h_j - h_0) - T_0(s_j - s_0) \quad (14)$$

The chemical exergy:

$$ex_j^{ch} = \sum_k x_k \left(ex_j^{ch} - RT_0 x_k \ln(x_k)\right) \quad (15)$$

where x_k, R and $\overset{ch}{ex}_j$ present the mass ratio within the mixture, gas constant and chemical specific exergy, respectively.

3.2. Methanol steam reforming

Since hydrogen and oxygen are the main components of fuel cells, methanol fuel cells require the installation of a methanol steam reforming system. In this system, hydrogen will be produced by heating, reforming, and combining the aqueous and methanol processes. It is possible to summarize the main chemical process as follows:

Endothermic reaction:

$$CH_3OH + H_2O \rightarrow CO_2 + 3H_2 \quad \triangle H_{298.15} = +49.4\ kJ/mol \quad (16)$$

Decomposion reaction of methanol (to produce hydrogen):

$$CH_3OH \rightarrow CO + 2H_2 \quad \triangle H_{298.15} = +90.5\ kJ/mol \quad (17)$$

The water-gas-shift reaction (to produce hydrogen):

$$CO + H_2O \rightarrow CO_2 + H_2 \quad \triangle H_{298.15} = -41.1\ kJ/mol \quad (18)$$

Catalysts are used to speed up reactions while also ensuring their direction and processing. CuO/ZrO_2 has been chosen in this scenario (Purnama et al., 2004)(Faungnawakij et al., 2006).

After reforming, oxygen and hydrogen are sent to the fuel cell cathode and anode, respectively. Following is a summary of the chemical reaction between the anode and cathode:

$$H_2 \rightarrow 2H^+ + 2e^- \quad (19)$$

$$O_2 + 4H^+ + 4e^- \rightarrow 2H_2O \quad (20)$$

The overall reaction:

$$2H_2 + O_2 \rightarrow 2H_2O \quad (21)$$

The methanol stream reformer will minimize its overall Gibbs energy in order to bring methanol into thermodynamic equilibrium (Ishak et al., 2012):

$$(\triangle G_{system})_{T,P} = 0 \quad (22)$$

Gibbs free energy (Authayanun et al., 2012) can be estimated by:

$$G_{system} = \left(\sum n_i \left[\overset{-0}{g}_{fi} + RT\ln(y_i P)\right]\right)_{gas} + \left(\sum n_i \overset{-0}{g}_{fi}\right)_{condensed} \quad (23)$$

$$\min_{nj}(G_{MSR})_{T,p} = \min_{nj}\left(\sum_{j=1}^{k} n_j \overline{G}_j\right)\sum_{j=1}^{k} n_j\left(G_j^0 + RTln\frac{\overline{f}_j}{f_j^0}\right) \quad (24)$$

Due to the conversion of atomic species:

$$\sum_{j=1}^{k} n_j a_{j,d} = b_d \qquad \text{for } 1 \le d \le D \quad (25)$$

The production of hydrogen:

$$y_{H_2} = \frac{\dot{F}_{H_2,out}}{\dot{F}_{Methanol,\ out}} \times \frac{1}{3} \times 100\% \quad (26)$$

3.3. Model of the SOFC

- Fuel and oxidant utilization

Based on the actual supply and consumption of methanol or its hydrogen counterpart, the usage of methanol can be approximated (Zhou et al., 2022):

$$U_{fuel} = \frac{(Fuel)_{reacted}}{(Fuel)_{inlet}} = \frac{(H_2)_{reacted}}{(H_2)_{inlet}} \quad (27)$$

The air utilization as:

$$U_{f-air} = \frac{(Air)_{reacted}}{(Air)_{inlet}} = \frac{(O_2)_{reacted}}{(O_2)_{inlet}} \quad (28)$$

The oxygen flow provided to the cathode can be calculated through power produced by SOFC (P_{SOFC}) divided to the number of transfer electrons (n), Faraday constant - 96.458 (F) and the SOFC's voltage:

$$f_{SOFC,O_2} = \frac{P_{SOFC}}{V_{SOFC} \cdot n \cdot F}\left(\frac{mol}{\min}\right) \quad (29)$$

$$q_{fuel} = \frac{i \cdot N_{Cell} \cdot A_{Cell}}{U_f \cdot n \cdot F}\left(\frac{mol}{s}\right) \quad (30)$$

The hydrogen flow provided to the anode can be calculated through main reaction between hydrogen and oxygen at the cathode of SOFC:

$$f_{SOFC,\ H_2} = 2 \cdot f_{SOFC,\ O_2}\left(\frac{mol}{\min}\right) \quad (31)$$

The SOFC system's net power output can be computed using the component stack as follows: (Song et al., 2021) (Liu et al., 2019)(Chitgar and Moghimi, 2020):

$$W_{stack} = i.A.V_c\eta_{DA} \quad (32)$$

where i, A, η_{DA} and V_c are the current density (A/m^2), surface area (m^2), converter efficiency, and actual voltage of the stack (V) (Liu et al., 2019).

$$V_c = V_R - V_{loss} \quad (33)$$

where V_R is cell ideal reversible voltage and,

$$V_{loss} = V_{ohm} + V_{act} + V_{con} \quad (34)$$

In which, and are the ohmic losses (V), activation losses (V) and concentration losses (V), respectively.

$$V_{ohm} = V_{ohm,a} + V_{ohm,c} + V_{ohm,e} + V_{ohm,int} \quad (35)$$

$$V_{ohm,a} = \frac{i\rho_a\ (A.\pi.D_m)8.\ t_a}{} \quad (36)$$

$$V_{ohm,c} = \frac{i\rho_c\ (A.\pi.D_m)^2}{8.\ t_c}.\ A.\ (A+2(1-A-B)) \quad (37)$$

$$V_{ohm,e} = i\rho_a t_e \quad (38)$$

$$V_{ohm,int} = i.\ \rho_{int}.\pi.\ D_m\frac{t_{int}}{w_{int}} \quad (39)$$

$$V_{act} = \frac{2RT}{F.\ n_e}\ Arcsinh\left(\frac{i}{2i_{0,k}}\right) \quad (40)$$

$$V_{con} = \frac{RT}{2F}\ln\left(\frac{1-\frac{i}{i_{L,H_2}}}{1+\frac{i}{i_{L,O_2}}}\right) + \frac{RT}{2F}\ln\left(\frac{1}{1-\frac{i}{i_{L,O_2}}}\right) \quad (41)$$

Furthermore, the I-V curve can also be used to define the actual voltage of the stack (Milewski et al., 2021).

Alternatively, the fuel cell's energy efficiency can be computed as

$$\eta_{en,\ SOFC} = \frac{\dot{W}_{elect,SOFC}}{\dot{m}_2h_2 + \dot{m}_{air}h_{air} - \dot{m}_{11}h_{11}} \quad (42)$$

(Liu et al., 2019)(Mehrpooya et al., 2016):

$$\eta_{en,SOFC} = \frac{\dot{W}_{SOFC}}{\dot{m}_2 LHV_{fuel_2}} \quad (43)$$

where $\dot{m}_2$ denotes the mass flow rate of methanol enter the SOFC system (kg/h) and LHV_{fuel-2} is the low heating value of methanol (kj/kg).

3.4. Model of PEMFC

Due to its high power density, low emissions, environmental friendliness, low maintenance requirements, smooth and silent operation, and low emission levels, the PEMFC is a potential power producing device for marine applications (Faungnawakij et al., 2006). Based on its

operating performance, HT-PEMFC can be divided into two categories: HT-PEMFC and low-temperature PEMFC (Han et al., 2020)(Chen et al., 2022)(Dimitrovar and Nader, 2022) (Smith and Novy, 2019). HT-PEMFC, which normally works between 120 and 200 °C, has better waste heat and CO tolerance and is more appropriate for energy conversion devices than LT-PEMFC (Zhang et al., 2016). The current research focuses on HT-PEMFC, which has its own characteristics, as water production control and pure hydrogen quality are main challenges for PEMFC. The primary justifications for choosing HT-PEMFC include: i) Compared to LT-PEMFC, HT-PEMFC requires hydrogen of lower quality, and it can tolerate about 3% CO (Oh et al., 2014); ii) Water is not concerned because at the high working temperature of the HT-PEMFC, water is in the vapor state (Jiao and Li, 2011); iii) The HT-PEMFC shows better electrochemical kinetics than the LT-PEMFC; iv) Waste heat recovery is simpler and more efficient (Zhang et al., 2006)

- The power generated by PEMFC:

$$W_{stack,PEMFC} = N_{cell} \cdot V_{cell} \cdot i \cdot A_{cell} \quad (44)$$

$$Q_{stack,PEMFC} = W_{stack,PEMFC} \cdot \frac{(V_{rev} - V_{ave})}{V_{ave}} \quad (45)$$

The required hydrogen and air for PEMFC can be estimated (Marandi et al., 2021):

- Mass flow rate of hydrogen:

$$\dot{m}_{H_2,PEMFC} = \lambda_{anode} \cdot M_{H_2} \cdot \frac{N_{cell} \cdot i}{2F} = \lambda_{anode} \cdot M_{H_2} \cdot \frac{N_{cell} \cdot A_{cell} \cdot i}{2F} \quad (46)$$

- Mass flow rate of air:

$$\dot{m}_{air,PEMFC} = \lambda_{cathode} \cdot M_{air} \cdot \frac{N_{cell} \cdot i}{4F \cdot g_{O_2}} = \lambda_{cathode} \cdot M_{air} \cdot \frac{N_{cell} \cdot A_{cell} \cdot i}{4F \cdot g_{O_2}} \quad (47)$$

As heat control of the PEMFC, the heat provided to the evaporator as:

$$Q_{evaporator} = Q_{stack} - Q_{reaction} - Q \quad (48)$$

The entire efficiency of PEMFC:

$$\eta_{PEMFC} = \frac{\dot{W}_{PEMFC}}{\dot{m}_{H_2} LHV_{H_2}} \quad (49)$$

Thus,

$$\dot{W}_{PEMFC} = \eta_{PEMFC} \cdot \dot{m}_{H_2} \cdot LHV_{H_2} \quad (50)$$

The electrcal efficiency of PEMFC can also be estimated by the actual cell voltage:

$$\eta_{cell} = \frac{V}{1.25} \quad (51)$$

where 1.25 is the maximum OCV at vapor water product, V represents the actual cell voltage.

3.5. Model of the Gas Turbine system

The hot gaseous mixture expands as it reaches the gas turbine after leaving the afterburner, creating useful mechanical power. The exit temperature can be calculated using these equations:

$$T_{out} = T_{in} (PR)^{\frac{(k-1)}{k}} \quad (52)$$

The isentropic efficiency:

$$\eta_{s,T} = \frac{\sum_i (\dot{n}_i \bar{h}_i)_{in} - \sum_i (\dot{n}_i \bar{h}_i)_{out}}{\sum_i (\dot{n}_i \bar{h}_i)_{in} - \sum_i (\dot{n}_i \bar{h}_i)_{s,\ out}} \quad (53)$$

The exergy efficiency:

$$\psi_T = \frac{\dot{W}_T}{\sum_i (\dot{n}_i \overline{ex}_i)_{in} - \sum_i (\dot{n}_i \overline{ex}_i)_{out}} \quad (54)$$

The energy and exergy efficiency of the SOFC-GT:

Energy efficiency:

$$\eta_{en,SOFC,GT} = \frac{\dot{W}_{SOFC} + \dot{W}_{GT}}{\dot{m}_2 LHV_{fuel_2}} \quad (55)$$

Exergy efficiency:

$$\eta_{ex,SOFC,GT} = \frac{\dot{W}_{SOFC} + \dot{W}_{GT}}{\dot{m}_2 ex_{fuel_2}} \quad (56)$$

Air compressor

The process for calculating the gas turbine's isentropic energy and exergy efficiencies can also be used to determine the air compressor's isentropic efficiency:

$$\eta_{en,Compressor} = \frac{\sum_i (\dot{n}_i \bar{h}_i) s,_{out} - \sum_i (\dot{n}_i \bar{h}_i)_{in}}{\sum_i (\dot{n}_i \bar{h}_i)_{out} - \sum_i (\dot{n}_i \bar{h}_i)_{in}} \quad (57)$$

The air compressor's exergy efficiency:

$$\eta_{ex,Compressor} = \frac{\sum_i (\dot{n}_i \overline{ex}_i)_{in} - \sum_i (\dot{n}_i \overline{ex}_i)_{out}}{\dot{W}_C} \quad (58)$$

Electric generator

The excess power of electric generator:

$$\dot{W}_G = \eta_G \left(\dot{W}_T - \dot{W}_C\right) \quad (59)$$

Heat exchangers

The heat exchanger's hot and cold sources are determined by:

Hot source:

$$\dot{Q} = \sum_i \left(\dot{n}_i \bar{c}_{p,i}\right)_h \left(T_{h,in} - T_{h,out}\right) \quad (60)$$

Cold source:

$$\dot{Q} = \sum_i \left(\dot{n}_i \bar{c}_{p,i}\right)_h \left(T_{c,in} - T_{c,out}\right) \quad (61)$$

3.6. Organic Rankine cycle

For the CV and steady state condition, the ORC's energy conservation:

$$\dot{Q} + \sum \dot{m}_{in} h_{in} = \dot{W} + \sum \dot{m}_{out} h_{out} \quad (62)$$

ORC input energy:

$$\dot{Q}_{in,\ ORC} = \dot{m}_{ORC}\left(h_{27} - h_{28}\right) \quad (63)$$

ORC net electric power:

$$\dot{W}_{net,\ ORC} = \dot{W}_{ORC,\ Turbine} - \dot{W}_{ORC,\ Pump} \quad (64)$$

Energy efficiency of the ORC:

$$\eta_{en,\ ORC} = \frac{\dot{W}_{net,\ ORC}}{\dot{Q}_{net,ORC}} \quad (65)$$

Exergy efficiency of ORC :

$$\eta_{ex,\ ORC} = \frac{\dot{W}_{net,ORC}}{\dot{E}x_{net,ORC}} \quad (66)$$

The main components' exergy destruction rates are determined and displayed in Table 1.

Table 1 Exergy destruction of main components

Components	Exergy destruction rate	
SOFC	$\dot{E}x_2 + \dot{E}x_7 + \dot{E}x_{11-1} - \dot{E}x_{11} - \dot{W}_{SOFC} = \dot{E}x_{des}$	(67)
Afterburner	$\dot{E}x_{11} - \dot{E}x_{12} = \dot{E}x_{des}$	(68)
Gas Turbine	$\dot{E}x_{12} - \dot{E}x_{13} - \dot{W}_{Gas\ turbine} = \dot{E}x_{des}$	(69)
HEX-1	$\dot{E}x_{13} + \dot{E}x_7 - \dot{E}x_{14} - \dot{E}_8 = \dot{E}x_{des}$	(70)
HEX-2	$\dot{E}x_2 + \dot{E}x_{14} - \dot{E}x_{15} - \dot{E}_4 = \dot{E}x_{des}$	(71)
HEX-3	$\dot{E}x_{15} + \dot{E}x_3 - \dot{E}x_{16} - \dot{E}_{21} = \dot{E}x_{des}$	(72)
HEX-4	$\dot{E}x_{16} + \dot{E}x_{19} - \dot{E}x_{17} - \dot{E}x_{20} = \dot{E}x_{des}$	(73)
HEX-5	$\dot{E}x_{27} + \dot{E}x_{34} - \dot{E}x_{28} - \dot{E}_{31} = \dot{E}x_{des}$	(74)
PEMFC	$\dot{E}x_{24} + \dot{E}x_{25} - \dot{E}x_{27-2} - \dot{E}_{out} = \dot{E}x_{des}$	(75)
ORC turbine	$\dot{E}x_{31} - \dot{E}x_{32} - \dot{W}_{O_{Turbine}} = \dot{E}x_{des}$	(76)

The total energy and exergy efficiencies of combined system (Al-Hamed and Dincer, 2021)(Gholamian and Zare, 2016)(Meng et al., 2022):

Energy efficiency:

$$\eta_{\frac{en,}{all}} = \frac{\dot{W}_{elec,total}}{\dot{m}_1\ LHV_{Methanol}} \quad (77)$$

where $\dot{W}_{elec,total}$ is the net power production subtract consumption of the system:

$$\begin{aligned}\dot{W}_{elec,total} = {} & \dot{W}_{elec,SOFC} + \dot{W}_{Gasturbine} \\ & + \dot{W}_{\mathrm{Expander\ 1}} + \dot{W}_{PEMFC} \\ & + \dot{W}_{ORC,turbine} - \dot{W}_{Air\ comp} \\ & - \dot{W}_{ORC,pump}\end{aligned} \quad (78)$$

is lower heating value of methanol (kJ/kg)

Exergy efficiency:

$$\eta_{ex,total} = \frac{\dot{W}_{elec,total}}{\dot{m}_1\ ex_{Methanol}} \quad (79)$$

4. Simulation materials

Methanol was proposed to be the fuel for the SOFC-GT-PEMFC-ORC system, and ASPEN-HYSYS V12.1 (Aspen Tech, USA), which offers reliable methodology and a sizable database for computing physical attributes, was used to model the system. The Aspen Physical Property System REFPROP function was used in the simulation. The thermodynamic characteristics of the stream compositions and operating circumstances for the SOFC-GT-PEMFC-ORC integrated system's components were estimated by participating in the the Peng-Robinson (PR) equation of states

The boundary condition is demonstrated in Table 2 (Ezzat and Dincer, 2020)

Table 2 The designation parameters of SOFC combined system

Component	Parameter	Unit	Value
Fuel and air input conditions	Temperature of methanol	℃	25
	Pressure of methanol	bar	4
	Air components		79% N_2,

			21%O_2
	Heat exchange minimum approach temperature	℃	5
SOFC	Operating Pressure	bar	3.9
	Operating Temperature	℃	869.5
	Ambient pressure	bar	1.013
	Ambient temperature	℃	27
	Number of single cells		16523
	Fuel cell current density	A/m^2	1490
	Active surface area	m^2	0.21
	Hydrogen stoichiometric		1.2
	Oxygen stoichiometric		2
	Fuel utilization factor in SOFC		86%
	Anode thickness	cm	0.0011
	Cathode thickness	cm	0.0011
	Electrolyte thickness	cm	0.003
PEMFC	Operating pressure	bar	1.2
	Operating temperature	℃	167.7
	Number of single cells		7138
	Cell active area	m^2	0.06
	Current density	A/m^2	4350
	Hydrogen stoichiometric		1.2
	Oxygen stoichiometric		2
	Membrane hydration		24
	Membrane thickness	cm	0.011
Compressor	Isentropic efficiency	%	87
Expanders	Isentropic efficiency	%	90
Converter	DC-AC converter efficiency	%	98
Pumps	Isentropic efficiency	%	87

5. Modeling verification

Table 3 presents the modelling results of the designed model with methanol as the fuel, which were calculated using this study's proposal and results from the literature (Duong et al., 2022a). The estimated values correspond to the data from the literature, and the difference between the current simulation data and the literature data is kept within a reasonable range.

Table 3 Comparison between the simulation results from the suggested integrating model and the equivalent values from the literature

Parameter	Modelling	Reported (Duong et al., 2022a)	Different (%)
SOFC temperature (°C)	869.5	857.8	1.36
Gas Turbine inlet temperature (°C)	1137	1192	4.61
Cell voltage (V)	0.75	0.71	5.6
Current Density (A/m^2)	1490	1430	4.1
SOFC efficiency	57.29	56.8	0.49

The suggested system has the capacity to concurrently power the propulsion system and other electrical devices while also producing hot water for shipboard crew members. Subsystem is required because the subsystem generates 33.32% of the total power of the integrated system.

6. Results and discussions

6.1. Thermodynamic performances of the system

To accommodate the demands of the primary propulsion system, auxiliary machinery, maneuvering schedule, and seafarers, the vessels need 3800 kW of electrical power. The proposed system's energy efficiency and SOFC fuel utilization factor were calculated to be 57.29% and 0.83, respectively. The vessels require 3800 kW of electrical power to meet the needs of the main propulsion system, auxiliary equipment, maneuvering schedule, and seafarers' requirements. Four different power sources, including ORC, gas turbine, PEMFC and SOFC, are used to contribute of total output power. The subsystems operate the proposed system as anticipated because they produce 33.32% to the total power while the SOFC generates 66.68% of it.

The power produced and consumed by system are demonstrated in Table 4

Table 4 Power generated by main components of system

Component	Power output (kW)	Power consumption (kW)
SOFC	3800	-
PEMFC	1152	-
GT	700	-
ORC Turbine	27.41	-
Expander 1	20	-
Air Compressor	-	601.8
ORC Pump	-	2.796
Water Pump	-	0.1338

When considering the full system shown in Tables 3 and 4, the SOFC-GT subsystem can supply the marine propulsion plant with 4500 kW, or 78.95% of the system's total power output. The thermodynamic performances of system are calculated by equations (1) to (79) and presented in Table 5.

Table 5 Thermodynamic performances of the systems

Subsystem	Energy efficiency	Exergy efficiency
SOFC-GT	68.58	27.89
ORC	13.22	56.87
PEMFC-ORC	46.53	40.89
Total System	76.2	30.3

It is intriguing to learn that the PEMFC-ORC subsystem operates with high energy efficiency when part of an integrated system. PEMFC-ORC is predicted to have an energy and exergy efficiency of 46.53% and 40.89%, respectively.

An examination of the exergy degradation rates linked to the internal thermal processes that take place in the main system components is shown in Fig 2. The SOFC and gas turbine have the two largest exergy destruction rates, at 2199 kW and 1631.88 kW, respectively. The gas turbine may have more room for advancement than other machine parts, due to the high exergy loss rate. The third component is the PEMFC, which produces 1189.23 kW of power. The afterburner follows with a 1125.97 kW power output. Because of its higher entropy production at lower temperatures and steady heat transfer rate, the HEX-5 demonstrates the least amount of exergy destructions.

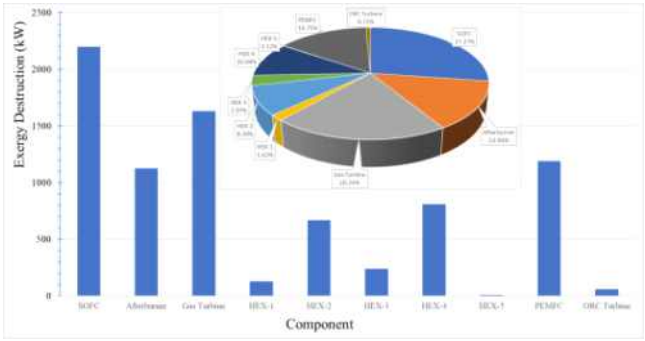

Fig. 2 Exergy desptructions of main components

The thermodynamics properties of each node of the system are depicted in Table 6.

Table 6 The detail properties of each stated node

Node	Vapor Fraction	Temp.	Pressure	Molar Flow	Liquid Volume Flow	Mass Enthalpy
Unit		C	kPa	kgmole/h	m^3/h	kJ/kg
1	0.00	25.00	403.00	37.07	1.49	-7548.59
2	0.00	25.00	403.00	31.51	1.27	-7548.59
3	0.00	25.00	403.00	5.56	0.22	-7548.59
4	1.00	450.00	396.11	31.51	1.27	-5490.12
5	1.00	147.45	396.11	126.03	4.41	-7559.48
6	1.00	27.00	101.30	450.10	15.01	1.74
7	1.00	189.34	400.00	450.10	15.01	168.59
8	1.00	492.60	396.55	450.10	15.01	495.48
9	1.00	437.71	94.43	605.53	20.40	-376.89
10	1.00	869.55	94.43	587.95	19.52	-376.89
11	1.00	869.55	94.43	558.55	18.54	-376.89
11-1	1.00	869.55	94.43	29.40	0.98	-376.89
12	1.00	1137.13	94.43	547.87	18.01	-376.89
13	1.00	1011.38	58.00	547.87	18.01	-549.93
14	1.00	794.74	51.11	547.87	18.01	-841.42
15	1.00	686.10	16.63	547.87	18.01	-984.12
16	1.00	670.80	9.74	547.87	18.01	-1004.02
17	1.00	495.38	2.84	547.87	18.01	-1228.26
18	0.00	27.00	100.00	63.01	1.14	-15879.19
19	0.00	27.03	420.00	63.01	1.14	-15878.77
20	1.00	250.00	416.55	63.01	1.14	-13002.16
20-1	1.00	250.00	416.55	31.51	0.57	-13002.16
20-2	1.00	250.00	416.55	31.51	0.57	-13002.16
21	1.00	250.00	399.55	5.56	0.22	-5922.04
22	1.00	292.43	399.55	48.19	1.25	-10774.36
23	1.00	292.81	399.55	17.61	0.48	-6334.50

24	1.00	155.81	120.00	17.61	0.48	-7269.58
25	1.00	28.00	140.00	152.90	5.10	2.65
26	1.00	47.60	120.00	179.41	5.87	-122.13
27	1.00	167.74	120.00	169.19	5.51	-122.13
28	1.00	34.41	113.11	169.19	5.51	-271.55
31	1.00	115.00	3010.53	30.00	2.99	-6567.87
32	0.96	34.92	480.00	30.00	2.99	-6591.97
33	0.00	32.00	445.53	30.00	2.99	-6734.13
34	0.00	34.25	3045.00	30.00	2.99	-6731.67
35	0.00	22.00	100.00	800.00	14.44	-15900.76
36	0.00	31.36	93.11	800.00	14.44	-15860.38

6.2. Effect of δ-parameter

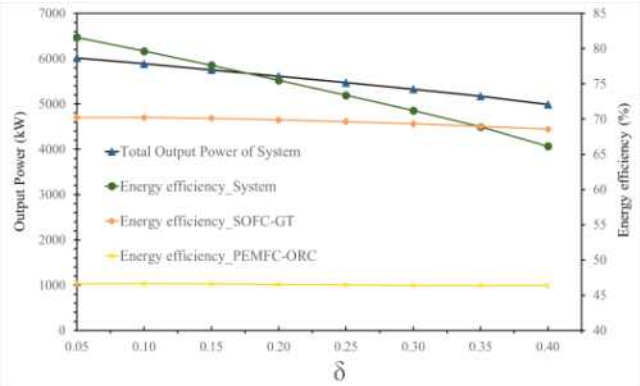

Fig. 3 Influence of δ-parameter to the power generation

The δ-parameter is defined as the ratio of methanol supplied to the H_2 generation and PEMFC systems to the total amount of methanol provided to entire system $\delta = \frac{\dot{m}_3}{\dot{m}_1}$. The δ-parameter was set to 0.14 in the simulation's basic scenario, which is adequate to drive the PEMFC system and produce 1152 kW of output power for the entire system. The entire energy and exergy efficiency of the system reduces as the ratio rises from 0 to 0.4. Fig 3 shows how the system's primary power generation components, including the PEMFC, change their power output in response to various values of the parameter.

According to Fig 3, when the ratio increased from 0 to 0.4, the SOFC power reduced from 4256.07 to 2688.74 kW while the PEMFC output power grew from 950.78 to 1604.85 kW. As a result, the total output power generated by the system decreased from 6018.25 to 4991.98 kW. It can be explained by the fact that the mass flow rates of hydrogen to PEMFC and SOFC are diverging, respectively. Additionally, it has led to the alteration of waste heat recovery systems and parts in compliance with SOFC and PEMFC. The output of GT decreases as SOFC exhaust gas reduction increases, and vice versa. As demonstrated in equations (77) and (78), the energy efficiency of system is effected by power generation and power consumption of system. So, δ parameter increased from 0.05 to 0.4 resulted to decrease energy efficiency of SOFC-GT and PEMFC-ORC subsystem from 70.23 to 68.58% and 46.62 to 46.38%, respectively.

Figs 4 illustrate influences of δ parameter to the exergy performances of entire system and subsystems.

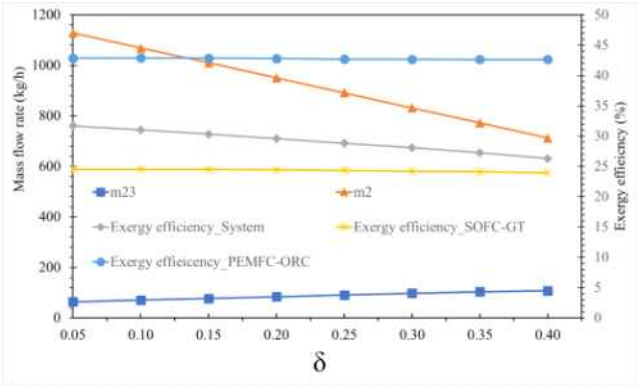

Fig. 4 Influence of δ parameter to exergy efficiency of the system

As the δ parameter grows, it becomes slightly less exerrgetic. This is a result of the devices' reduced power output, especially for SOFC and GT, as depicted in Fig 3. However, as seen in Fig 4, some component exergy rose as the parameters increased. The exergy of SOFC-GT is reduced from 31.71% to 26.30% with an increase of from 0 to 0.4, whereas the exergy efficiency of PEMFC is marginally enhanced from 42.87% to 42.65%.

7. Conclusions

Methanol is used as the primary fuel in a system that incorporates SOFC-GT-PEMFC-ORC to provide electricity for the ship's primary propulsion system and harvest high-temperature exhaust heat from SOFCs to generate surplus electricity for start-up, maneuvering, and accommodating seafarers. The designated multigenerational energy system intends to provide marine vessels with alternative, environmentally sound options by utilizing

renewable, sulfur-free, and low-carbon fuels in power plants. Energy and exergy assessments as well as thorough parametric research were carried out to evaluate the proposed system's performance and energy harvesting. The following are some of the study's most crucial conclusions:

- This study suggested a brand-new integrated system for use in marine vessels that will get through the main obstacle to SOFC application during start-up and maneuvering. In comparison to SOFC stand-alone systems, the integrated system increases 18.91% of efficiency, the total energy and exergy performance was calculated to be 76.02% and 30.3%, respectively. The system received 1880.3 kW from the GT-PEMFC-ORC, or accounted for 33.1% of the system's total power supply.

- The SOFC power was reduced from 4256.07 to 2688.74 kW when the mathanol distribution ratio (δ) was ranged from 0.05 to 0.4, and the PEMFC output power grew from 950.78 to 1604.85 kW. The system's energy efficiency has marginally decreased from 31.71% to 26.3%.

Acknowledgement

This research was supported by Korea Institute of Marine Science & Technology Promotion(KIMST) funded by the Ministry of Oceans and Fisheries, Korea(20200520).

This research was supported by BB21plus, funded by Busan Metropolitan City and Busan Institute for Talent and Lifelong Education (BIT).

This research is the winner of the Marine Fisheries Future Risk Paper Contest sponsored by the Korea Maritime Institute(KMI).

References

[1] Adamson, K. A. and Pearson, P.(2000), "Hydrogen and methanol: A comparison of safety, economics, efficiencies and emissions", J. Power Sources, Vol. 86, pp. 548-555.

[2] Al-Hamed, K. H. M. and Dincer, I.(2021), "A novel ammonia solid oxide fuel cell-based powering system with on-board hydrogen production for clean locomotives", Energy, Vol. 220, No. 119771.

[3] Al-Hamed, K. H. M. and Dincer, I.(2019), "A new direct ammonia solid oxide fuel cell and gas turbine based integrated system for electric rail transportation", eTransportation, Vol. 2, No. 100027.

[4] Alias, M. S., Kamarudin, S. K., Zainoodin, A. M. and Masdar, M. S.(2020), "Active direct methanol fuel cell: An overview", Int. J. Hydrogen Energy, Vol. 45, pp. 19620-19641.

[5] Ashrafi, M., Lister, J. and Gillen, D.(2022), "Toward a harmonization of sustainability criteria for alternative marine fuels", Marit. Transp. Res., Vol. 3, No. 100052.

[6] Atacan, O. F., Ouellette, D. and Colpan, C. O.(2017), "Two-dimensional multiphase non-isothermal modeling of a flowing electrolyte - Direct methanol fuel cell", Int. J. Hydrogen Energy, Vol. 42, pp. 2669-2679.

[7] Authayanun, S., Mamlouk, M. and Arpornwichanop, A.(2012), "Maximizing the efficiency of a HT-PEMFC system integrated with glycerol reformer", Int. J. Hydrogen Energy, Vol. 37, pp. 6808-6817.

[8] Bicer, Y. and Khalid, F.(2020), "Life cycle environmental impact comparison of solid oxide fuel cells fueled by natural gas, hydrogen, ammonia and methanol for combined heat and power generation", Int. J. Hydrogen Energy, Vol. 45, pp. 3670-3685.

[9] Calabriso, A., Cedola, L., Del Zotto, L., Rispoli, F. and Santori, S. G.(2015), "Performance investigation of Passive Direct Methanol Fuel Cell in different structural configurations", J. Clean. Prod., Vol. 88, pp. 23-28.

[10] Chen, C. C., Jeng, M. S., Leu, C. H., Yang, C. C., Lin, Y. L., King, S. C. and Wu, S. Y.(2011), "Low-level CO in hydrogen-rich gas supplied by a methanol processor for PEMFCs", Chem. Eng. Sci., Vol. 66, pp. 5095-5106.

[11] Chen, H., Liu, Z., Ye, X., Yi, L., Xu, S. and Zhang, T., (2022), "Air flow and pressure optimization for air supply in proton exchange membrane fuel cell system", Energy, Vol. 238, No. 121949.

[12] Chitgar, N. and Moghimi, M.(2020), "Design and evaluation of a novel multi-generation system based on SOFC-GT for electricity, fresh water and hydrogen production", Energy, Vol. 197, No. 117162.

[13] Dimitrovar, Z. and Nader, W. B.(2022), "PEM fuel cell as an auxiliary power unit for range extended hybrid electric vehicles", Energy Vol. 239, No. 121933.

[14] Duong, P. A., Ryu, B., Jung, J. and Kang, H.(2022a), "Thermal Evaluation of a Novel Integrated System Based on Solid Oxide Fuel Cells and Combined Heat and Power Production Using Ammonia as Fuel", Appl. Sci. Vol. 12, No. 6287.

[15] Duong, P. A., Ryu, B., Kim, C., Lee, J. and Kang, H. (2022b), "Energy and Exergy Analysis of an Ammonia Fuel Cell Integrated System for Marine Vessels",

Energies, Vol. 15, Issue. 9.

[16] Ezzat, M. F. and Dincer, I.(2020), “Energy and exergy analyses of a novel ammonia combined power plant operating with gas turbine and solid oxide fuel cell systems”, Energy, Vol. 194, No. 116750.

[17] Faungnawakij, K., Kikuchi, R. and Eguchi, K.(2006), “Thermodynamic evaluation of methanol steam reforming for hydrogen production”, J. Power Sources, Vol. 161, pp. 87-94.

[18] Gholamian, E. and Zare, V.(2016), “A comparative thermodynamic investigation with environmental analysis of SOFC waste heat to power conversion employing Kalina and Organic Rankine Cycles”, Energy Convers. Manag., Vol. 117, pp. 150-161.

[19] Han, Jaeyoung, Han, Jaesu and Yu, S.(2020). “Investigation of FCVs durability under driving cycles using a model-based approach”, J. Energy Storage, Vol. 27, No. 101169.

[20] Hansson, J., Brynolf, S., Fridell, E. and Lehtveer, M.(2020). The potential role of ammonia as marine fuel-based on energy systems modeling and multi-criteria decision analysis. Sustain. Vol. 12, pp. 10-14. https://doi.org/10.3390/SU12083265

[21] International Maritime Organzation, n.d. Adoption of the Initial IMO Strategy on Reduction of GHG Emissions from Ships Vol. 10.

[22] Ishak, F., Dincer, I. and Zamfirescu, C.(2012), “Thermodynamic analysis of ammonia-fed solid oxide fuel cells”, J. Power Sources, Vol. 202, pp. 157-165.

[23] Jiao, K. and Li, X.(2011), “Water transport in polymer electrolyte membrane fuel cells”, Prog. Energy Combust. Sci., Vol. 37, pp. 221-291.

[24] Kim, T., Ahn, K., Vohs, J. M. and Gorte, R. J.(2007), “Deactivation of ceria-based SOFC anodes in methanol”, J. Power Sources, Vol. 164, pp. 42-48.

[25] Kulikovsky, A. A.(2008), “Optimal temperature for DMFC stack operation”, Electrochim. Acta, Vol. 53, pp. 6391-6396.

[26] Laosiripojana, N. and Assabumrungrat, S.(2007), “Catalytic steam reforming of methane, methanol, and ethanol over Ni/YSZ: The possible use of these fuels in internal reforming SOFC”, J. Power Sources Vol. 163, pp. 943-951.

[27] Li, R., Liu, Y. and Wang, Q.(2022), “Emissions in maritime transport: A decomposition analysis from the perspective of production-based and consumption-based emissions”, Mar. Policy, Vol. 143, No. 105125.

[28] Li, Y., Li, D., Ma, Z., Zheng, M., Lu, Z., Song, H. and Guo, X.(2022), “Performance analysis and optimization of a novel vehicular power system based on HT-PEMFC integrated methanol steam reforming and ORC”, Energy, Vol. 257, No. 124729.

[29] Liu, Y., Han, J. and You, H.(2019), “Performance analysis of a CCHP system based on SOFC/GT/CO2 cycle and ORC with LNG cold energy utilization”, Int. J. Hydrogen Energy, Vol. 44, pp. 29700-29710.

[30] Marandi, S., Sarabchi, N. and Yari, M.(2021), “Exergy and exergoeconomic comparison between multiple novel combined systems based on proton exchange membrane fuel cells integrated with organic Rankine cycles, and hydrogen boil-off gas subsystem”, Energy Convers. Manag., Vol. 244, No. 114532.

[31] Mehrpooya, M., Dehghani, H. and Ali Moosavian, S.M.(2016), “Optimal design of solid oxide fuel cell, ammonia-water single effect absorption cycle and Rankine steam cycle hybrid system”, J. Power Sources Vol. 306, pp. 107-123.

[32] Meng, T., Cui, D., Ji, Y., Cheng, M. and Tu, B.(2022), “Optimization and efficiency analysis of methanol SOFC-PEMFC hybrid system”, Int. J. Hydrogen Energy, Vol. 47, Issue. 64, pp. 27690-27702.

[33] Milewski, J., Szczęśniak, A. and Szabłowski, Ł.(2021), “A proton conducting solid oxide fuel cell－implementation of the reduced order model in available software and verification based on experimental data”, J. Power Sources Vol. 502.

[34] Oh, K., Jeong, G., Cho, E., Kim, W. and Ju, H.(2014), “A CO poisoning model for high-temperature proton exchange membrane fuel cells comprising phosphoric acid-doped polybenzimidazole membranes”, Int. J. Hydrogen Energy, Vol. 39, Issue. 36, pp. 21915-21926.

[35] Özcan, O. and Akın, A. N.(2019), “Thermodynamic analysis of methanol steam reforming to produce hydrogen for HT-PEMFC: An optimization study”, Int. J. Hydrogen Energy, Vol. 44, Issue. 27, pp. 14117-14126.

[36] Purnama, H., Girgsdies, F., Ressler, T., Schattka, J. H., Caruso, R. A., Schomäcker, R. and Schlögl, R.(2004), “Activity and selectivity of a nanostructured CuO/ZrO2 catalyst in the steam reforming of methanol”, Catal. Letters, Vol. 94, pp. 61-68.

[37] Sankar, K., Thakre, N., Singh, S. M. and Jana, A. K.(2017), “Sliding mode observer based nonlinear

control of a PEMFC integrated with a methanol reformer", Energy Vol. 139, pp 1126-1143.

[38] Smith, J. D. and Novy, M.(2019), "Design of a Modern Proton-Exchange Membrane Fuel Cell Module for Engineering Education", 2018 IEEE Conf. Technol. Sustain. SusTech 2018.

[39] Song, M., Zhuang, Y., Zhang, L., Li, W., Du, J. and Shen, S.(2021), "Thermodynamic performance assessment of SOFC-RC-KC system for multiple waste heat recovery" Energy Convers. Manag. Vol. 245, No. 114579.

[40] Valera-Medina, A., Amer-Hatem, F., Azad, A.K., Dedoussi, I.C., De Joannon, M., Fernandes, R.X., Glarborg, P., Hashemi, H., He, X., Mashruk, S., McGowan, J., Mounaim-Rouselle, C., Ortiz-Prado, A., Ortiz-Valera, A., Rossetti, I., Shu, B., Yehia, M., Xiao, H. and Costa, M.(2021), "Review on ammonia as a potential fuel: From synthesis to economics", Energy and Fuels, Vol. 35, pp. 6964-7029.

[41] Wang, C., Li, Y., Xu, C., Badawy, T., Sahu, A. and Jiang, C.(2019), "Methanol as an octane booster for gasoline fuels", Fuel, Vol. 248, pp. 76-84.

[42] Wang, X., Yuen, K. F., Wong, Y. D. and Li, K. X.(2020), "How can the maritime industry meet Sustainable Development Goals? An analysis of sustainability reports from the social entrepreneurship perspective", Transp. Res. Part D Transp. Environ., Vol. 78, No. 102173.

[43] Xing, H., Stuart, C., Spence, S. and Chen, H.(2021), "Alternative fuel options for low carbon maritime transportation: Pathways to 2050", J. Clean. Prod. Vol. 297, No. 126651.

[44] Zhang, C., Liu, Z., Zhang, X., Chan, S. H. and Wang, Y.(2016), "Dynamic performance of a high-temperature PEM (proton exchange membrane) fuel cell - Modelling and fuzzy control of purging process", Energy, Vol. 95, pp. 425-432.

[45] Zhang, Jianlu, Xie, Z., Zhang, Jiujun, Tang, Y., Song, C., Navessin, T., Shi, Z., Song, D., Wang, H., Wilkinson, D. P., Liu, Z. S. and Holdcroft, S.(2006), "High temperature PEM fuel cells", J. Power Sources, Vol. 160, pp. 872-891.

[46] Zhang, P., Yang, Y., Yang, Z. and Peng, S.(2022), "Direct power generation from methanol by solid oxide fuel cells with a Cu-ceria based catalyst layer", Renew. Energy, Vol. 194, pp. 439-447.

[47] Zhao, J., Cai, S., Luo, X. and Tu, Z.(2022), "Dynamic characteristics and economic analysis of PEMFC-based CCHP systems with different dehumidification solutions", Int. J. Hydrogen Energy, Vol. 47, pp 11644-11657.

[48] Zhou, J., Wang, Z., Han, M., Sun, Z. and Sun, K.(2022), "Optimization of a 30 kW SOFC combined heat and power system with different cycles and hydrocarbon fuels", Int. J. Hydrogen Energy, Vol. 47, pp. 4109-4119.

[49] Zis, T. P. V., Psaraftis, H. N., Tillig, F. and Ringsberg, J. W.(2020), "Decarbonizing maritime transport: A Ro-Pax case study", Res. Transp. Bus. Manag., Vol. 37.

Received 10 November 2022
Revised 20 February 2023
Accepted 20 February 2023